EMISSION OF AN ATMOSPHERIC PRESSURE ARC IN A GAS FLOW

E.A. ERSHOV-PAVLOV*, K.L. STEPANOV, Yu.A.STANKEVICH, L.K.STANCHITS

Heat & Mass Transfer Institute, 15, P. Brovka str., 220072 Minsk, Belarus
E-mail: kls@hmti.ac.by
*Institute of Molecular & Atomic Physics, 70, F. Scaryna Ave., 220072 Minsk, Belarus
E-mail: ershov@imaph.bas-net.by

Abstract. Techniques and results are presented of the emission calculation for an atmospheric pressure arc stabilized with a gas flow. Local thermodynamic equilibrium (LTE) is used as an approximation for the arc positive column. Spectral (in visible and UV region), as well as total emission parameters are studied using the approximation for the arc plasma volume having two-dimensional temperature distribution of an axial symmetry. A radiative-collisional model is formulated for the arc near cathode region, where a departure from LTE is observed. The model accounts a population of excited particles on energy levels and the plasma emission. Air plasma is taken to fit for the analysis of the arcs in air and nitrogen gas flows.

Arc plasma parameters. The study is limited with positive columns and near cathode regions of transferred arcs. Here the plasma is mainly composed of the flow gas particles. Moreover, at a constant pressure the arc positive column is a stationary non-uniform plasma volume of an axial or conical geometry. Usually the arc axial gradient is much lower of the radial one even for the near cathode regions. A typical temperature distribution is shown in Fig. 1 for the transferred arc in nitrogen at 250 A current. (Megy, 1995).

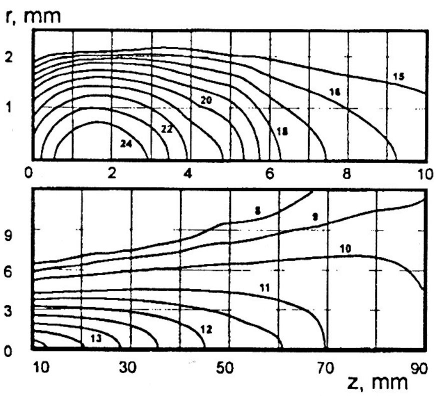

Fig. 1. Arc temperature distribution (kK).

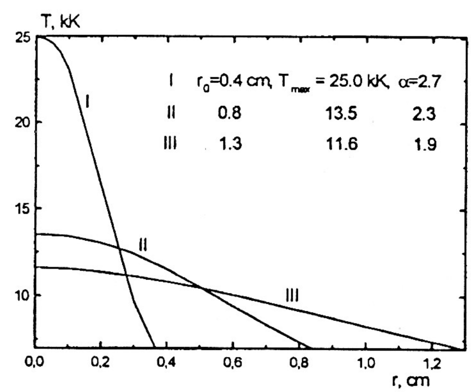

Fig. 2. Radial temperature profiles.

Radial temperature profiles of the arcs can be presented in a parametrical form, e.g., $T(r) = T_0\left[1 + A(r/r_0)^\alpha\right]^{-1}$ (Bousrih, 1995). Here T_0 is the plasma axial temperature, r_0 is the arc radius, α determins the temperature profile form (from a uniform at $\alpha \to \infty$ up to a very steep one, when $\alpha \sim 1$), $A = T_0 / T(r_0) - 1$. The temperature two-dimensional profile T(r,z) also can be easily presented with this expression, if one takes into account, that T_0, r_0, α and A depend on z. In Fig. 2 radial temperature profiles are shown for three axial positions (I - z = 0.16 cm, II - z = 2 and III - z = 6 cm) of the arc (Megy, 1995).

Radiation transfer calculations. Theoretical (Avilova, 1970, Romanov 1995) and experimental (Shimanovich, 1997) data on optical properties of air plasma have been used for the radiation transfer consideration. Measured spectral absorption coefficients are presented in Fig. 3 for atmospheric pressure air plasma at different temperatures (Shimanovich, 1997).

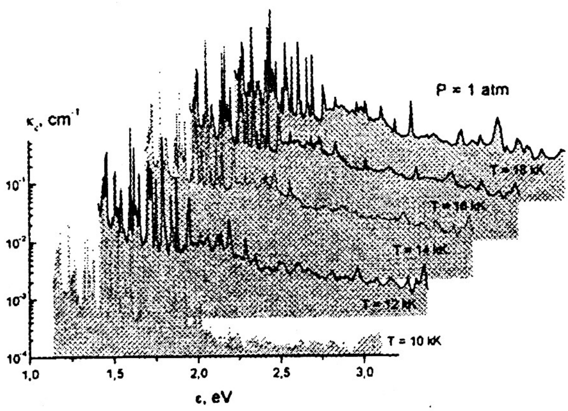

Fig. 3. Spectral absorption coefficients of air plasma at P= 1atm, T=10-18 kK.

The radiation transfer equation has been solved supposing two- or one-dimensional cylindrical geometry of the arc plasma volume for the temperature profiles, shown in Figs. 1, 2.

$$\left(\mu \frac{\partial I_\varepsilon}{\partial r} - \frac{1-\mu^2}{r}\frac{\partial I_\varepsilon}{\partial \mu}\right)\mathrm{Sin}\theta + \frac{\partial I_\varepsilon}{\partial z}\mathrm{Cos}\theta = \kappa_\varepsilon (I_{p\varepsilon} - I_\varepsilon). \quad (1)$$

The solution has been found along the eq.(1) characteristics, which correspond to Gauss knots of the angle variables determining the radiation flux from the plasma

$$d\Omega = d\chi\,\mathrm{Sin}\Psi\, d\Psi, \qquad \mathrm{Cos}\Psi = \mathrm{Sin}\theta\mathrm{Cos}\varphi, \qquad \mathrm{Sin}\psi\mathrm{Cos}\chi = \mathrm{Sin}\theta\mathrm{Sin}\varphi. \quad (2)$$

Taking into account the symmetry, the flux has been determined from a one-dimensional cylinder surface using the following expression

$$S_\varepsilon = 4\int_0^{\pi/2} d\chi \int_0^{\pi/2} \mathrm{Cos}\Psi\,\mathrm{Sin}\Psi\, I_\varepsilon(\chi,\psi)\, d\Psi = \frac{\pi^2}{4}\sum_i W_i \sum_j \mathrm{Cos}\Psi_j\,\mathrm{Sin}\Psi_j\, I_\varepsilon(\chi_i,\Psi_j)\, W_j, \quad (3)$$

(W_i are weights of the Gauss quadrature formulas) providing 64 rays pass in $\pi/2$ solid angle. Separately, radiation intensity has also been calculated in the plane normal to the cylinder axis and in the direction passing through the axis. At the integration (1) along the ray, the source function in a calculation cell has been approximated with the linear dependence.

$$I_\varepsilon(\tau_i) = I_\varepsilon(\tau_{i-1})e^{(-\Delta\tau_i)} + I_{p\varepsilon}(\tau_i)\left[1 - e^{(-\Delta\tau_i)}\right] - \left(\frac{dI_{p\varepsilon}}{d\tau}\right)_i \left[1 - e^{(-\Delta\tau_i)}(1 + \Delta\tau_i)\right], \quad (4)$$

It provided true asymptotics $I_\varepsilon(\tau_i)$ in small and large τ limits.

Emission of the arc positive column. Data on group (for 6 spectral intervals) and total radiation fluxes from the positive column surface of the arc are presented in Table 1.

Note the following. Inspite of the equilibrium emission maximum corresponding to axial temperatures is observed in the spectral interval $\varepsilon \approx 2.5 - 6$ eV, the plasma radiation flux in shorter wavelengths (groups 5 and 6) is rather important. It is due to the plasma large opacity in these spectral regions, as well as because of strong spectral lines, which totally determine the radiation output. In the visible region ($\varepsilon \approx 1.15$-4.5 eV) the flux falls with the plasma mean temperature decrease. At a time its part in the total flux increases up to 5.2, 25 и 35.5% for the profiles I, II, III, respectively. Total power (per length unit) decreases monotonously (6.3, 2.1 и 0.99 kW/cm). On the contrary in visible region of the spectrum the value increases to 0.25, 0.55 and 0.35 kW/cm, respectively.

Table 1. Radiation fluxes from the arc positive column, kW/cm^2

S, kW/cm^2							
Δε, eV	0.03-1.15	1.15-3.16	3.16-4.52	4.52-6.51	6.51-11	11-17	0-∞
Δλ, nm	>1078	1078-392	392-274	274-190	190-113	113-73	∞-0
I	$6.5\cdot10^{-2}$	$1.21\cdot10^{-1}$	$1.03\cdot10^{-2}$	$7.98\cdot10^{-3}$	$7.23\cdot10^{-1}$	1.58	2.51
II	$3.87\cdot10^{-2}$	$9.63\cdot10^{-2}$	$7.60\cdot10^{-3}$	$5.29\cdot10^{-3}$	$1.74\cdot10^{-1}$	$9.73\cdot10^{-2}$	$4.19\cdot10^{-1}$
III	$1.22\cdot10^{-2}$	$3.81\cdot10^{-2}$	$4.78\cdot10^{-3}$	$2.85\cdot10^{-3}$	$4.81\cdot10^{-2}$	$1.55\cdot10^{-2}$	$1.21\cdot10^{-1}$

Fig. 4 gives an idea about a role of different radial parts of the positive column in the output radiation formation. Here directed radiation intensity is shown in the points of the normal ray with $\xi = 0.5r_0, r_0, 1.5r_0, 2r_0$ (section II). One can see from the spectra comparison in the ray points at $0.5r_0$, r_0 и $2r_0$, that the emission in periphery layers of the column practically do not give any input in the radiation with $\varepsilon \leq 10$ eV energy. The same layers shield VUV radiation, which is generated in the column hot regions, with the radiation in free-bound continuum falling down up to the order and more of the value at the axis, and spectral lines are totally reabsorbed.

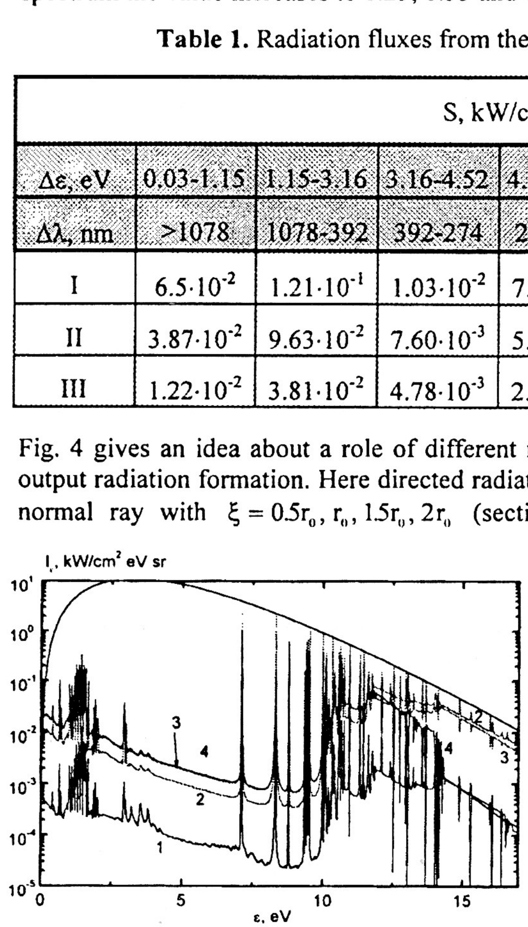

Fig. 4. Spectral intensity in different ray points.

Arc emission in the near-cathode region. The results above are based on the LTE approximation, that is limited for the plasma near the arc cathode region. Here at the space scale of the cathode spot dimension, temperatures of electrons and heavy particles can differ much, and the exited particles distribution on energy levels does not obligatory corresponds to the Boltzmann-Saha law. One of the evidence of the LTE deviation is an "unusual" behaviour of the maximum emissivity of atomic lines with the distance from the cathode, see, e.g, Haddad (1984), Pellerin (1992), Razafinimanana (1994) for argon and Megy (1995) for nitrogen plasmas. Closer to the cathode, the line emissivity maxima become lower, and the temperatures, at which they are observed, are higher. As a result it causes a difference in temperatures measured using atom and ion spectral lines (e.g., NI λ =746.8 nm and NII λ =399.5 nm, Megy, 1995). There are some processes which can cause the plasma state deviation of the equlibrium one near the cathode. We note the following possible important reasons: emission of non-termal electrons from the cathode, very high current density at the cathode tip, non-compensated spontaneous radiative decay of the excited levels.

We used radiative-collisional model (RCM) to account a population kinetics of the atomic excited levels and to evaluate the arc radiation in the near-cathode region. The kinetics equations content basical elementary acts and processes responsible for the level population (collisional ionization and triple recombination, excitation and de-excitation by electron impacts, radiative level decay, photo- and dielectron recombination).

Stationary approximation RCM (Romanov, 1991)

$$\sum_n K^{(i)}_{mn} N^{(i)}_n + D^{(i)}_m = 0 \tag{5}$$

corresponds to an instantaneous reaction of the populations on ambiant conditions (electron temperature T_e and density N_e) and accounts the collisional-radiative equilibrium states in a large interval of plasma parameters. In the limiting case of low and high densities coronal and thermodynamic equilibriums, respectively, are realized.

Results of our calculations using the model show, that for plasmas near the arc cathode (T~2 eV, N_e~(2-4)$\cdot 10^{17}$ cm^{-3}) there is a rather strong deviation from the equilibrium not only of the excited levels population, but also of the plasma charge composition. One can see a relative increase of the plasma electron density due to a difference in electron and heavy particle temperatures at a constant pressure, as well as an intensity fall of the atomic lines because of the excited levels de-population. So, the results show qualitatively the phenomena previously observed experimentally (Megy, 1995). The equilibrium deviation results in lower emission of the near-cathode arc parts, than one can expect for LTE plasmas with such high parameters.

References

Avilova I.V., Biberman L.M., Vorob'ev V.S. at al.: 1970, The Optical Properties of Hot Air. Moscow, Nauka.

Bousrih S., Megy S., Ershov-Pavlov E., and Baronnet J.-M.: 1995, Proc. ISPC-12, Minneapolis, **4**, 1819.

Haddad G.H. and Farmer A.J.: 1984, J. Phys. D: Appl. Phys., **17**, 1189.

Megy S., Ershov-Pavlov E., Baronnet J.-M.: 1995, J. Phys. D: Appl. Phys., **28**, 344.

Pellerin S., Musiol K., Pokrzywka B., Chapelle J.: 1994, J. Phys.D: Appl. Phys., **27**, 522.

Razafinimanana M., Gudzy P., Gleizes A. et al.: 1994, J. High Temp. Chem. Proc., **4**, 51.

Romanov G.S., Stankevich Yu.A., Stanchits L.K., and Stepanov K.L.: 1995, Int. J. Heat Mass Transfer, **38**, 545.

Romanov G.S., Stepanov K.L., Stanchits L.K.: 1991, J. of Applied Spectroscopy (in Russian), **54**, 825.

Shimanovich V., Ershov-Pavlov E., Azharonok V. et al.: 1997, Preprint of the Institute of Molecular & Atomic Physics, No4, Minsk.